Accepted Manuscript

Oscillatory networks of high-level mental alignment: A perspective-taking MEG study

R.A. Seymour, H. Wang, G. Rippon, K. Kessler

Please cite this article as: Seymour, R.A., Wang, H., Rippon, G., Kessler, K., Oscillatory networks of high-level mental alignment: A perspective-taking MEG study, *NeuroImage* (2018), doi: 10.1016/ j.neuroimage.2018.05.016.

Oscillatory Networks of High-Level Mental

Alignment: A Perspective-Taking MEG Study

Seymour, R.A[1,2,3]., Wang, H[1]., Rippon, G[1]., & Kessler, K[1].

[1]Aston Brain Centre, School of Life and Health Sciences, Aston University, Birmingham, B4 7ET. [2]ARC Centre of Excellence in Cognition and Its Disorders, Macquarie University, Sydney, Australia, 2109. [3]Department of Cognitive Science, Macquarie University, Sydney, Australia, 2109.

Correspondence: Klaus Kessler (k.kessler@aston.ac.uk)

School of Life and Health Sciences

Psychology, Aston Brain Centre

Aston University

Aston Triangle

Birmingham, B4 7ET

Phone: +44 (0)121 204 3187

19

20 **Highlights**

21 • Oscillatory basis of embodied perspective-taking investigated using MEG

22 • We replicate the crucial role of theta-band (3-6Hz) oscillations in perspective-taking

23 • Theta power localised to right temporo-parietal junction (rTPJ), lateral PFC and ACC

24 • Lateral PFC and ACC exert top-down influence (Granger causality) over rTPJ

25 • rTPJ increases its theta-band phase coupling to mentalizing and body schema networks

26

27 **Abstract**

28 Mentally imagining another's perspective is a high-level social process, reliant on

29 manipulating internal representations of the self in an embodied manner. Recently Wang et

30 al. (2016) showed that theta-band (3-7Hz) brain oscillations within the right temporo-parietal

31 junction (rTPJ) and brain regions coding for motor/body schema contribute to the process of

32 perspective-taking. Using a similar paradigm, we set out to unravel the extended functional

33 brain network in detail. Increasing the angle between self and other perspective was

34 accompanied by longer reaction times and increases in theta power within rTPJ, right lateral

35 pre-frontal cortex (PFC) and right anterior cingulate cortex (ACC). Using Granger-causality,

36 we showed that lateral PFC and ACC exert top-down influence over rTPJ, indicative of

37 executive control processes required for managing conflicts between self and other

38 perspectives. Finally, we quantified patterns of whole-brain phase coupling in relation to the

39 rTPJ. Results suggest that rTPJ increases its theta-band phase synchrony with brain regions

40 involved in mentalizing and regions coding for motor/body schema; whilst decreasing

41 synchrony to visual regions. Implications for neurocognitive models are discussed, and it is

42 proposed that rTPJ acts as a 'hub' to route bottom-up visual information to internal

43 representations of the self during perspective-taking, co-ordinated by theta-band oscillations.

44

Keywords

Introduction

Humans possess highly developed social skills that allow us to imagine what others might be experiencing, thinking or feeling to an extent not shared by other species (Tomasello et al. 2005). The question of what separates us from other species has been the subject of substantial research in comparative psychology and cognitive neuroscience, and while significant headway has been made with respect to what skills make us special (Call and Tomasello 1999; Povinelli et al. 2000; Frith and Frith 2007) and which parts of our brain have evolved to cope with sophisticated "mentalizing", i.e., reading of others' minds (Lieberman 2007; Van Overwalle and Baetens 2009), much less is known about the actual brain network dynamics that implement these social skills. Here we set out to investigate the large-scale, distributed but synchronised neural activity that gives rise to a person's understanding of another's visuospatial experience of the world: a process termed perspective taking.

Mentally imagining another's perspective is a high-level social process, but recent behavioural experiments suggest that perspective-taking is still grounded in the cortical posture and action representations of the observer. Using posture manipulations, several studies (Kessler and Rutherford 2010; Kessler and Thomson 2010; Surtees et al. 2013; Wang et al. 2016; Gooding-Williams et al. 2017) have shown that perspective-taking engages large parts of the neuronal bases of the body schema, i.e. the cortical correlates of the internal representation of the body (Coslett et al. 2008; Medina et al. 2009), in the form of a simulated rotation of the embodied self into another's orientation and perspective (Kessler and

4

70 Thomson 2010; Surtees et al. 2013; Wang et al. 2016). In other words, humans literally "put

71 themselves" into another's viewpoint to understand their perspective.

72

73 Note that such embodied perspective-taking must be distinguished from so-called perspective

74 *tracking*. While both processes involve judgements about another's perspective, perspective-

75 tracking, in contrast to perspective-taking, merely requires an observer to understand what

76 another can or cannot perceive (e.g. what is occluded and what is visible to them). The two

77 forms of perspective processing have been related to different developmental stages (Flavell

78 et al. 1981; Gzesh and Surber 1985; Moll and Tomasello 2006)

79 (perspective-tracking: ~2 years; perspective-taking ~ 4-5 years) and perspective-tracking, in

80 contrast to perspective-taking, has been observed in other species such as apes and corvids

81 (Bugnyar et al. 2004; Bräuer et al. 2007). Finally, while perspective-taking engages an

82 embodied mental rotation of the self into another's viewpoint, perspective-tracking seems to

83 rely on inferring another's line of sight, in other words, whether their line of sight towards a

84 target is disrupted or not (Zacks and Michelon 2005; Kessler and Rutherford 2010; Wang et

85 al. 2016).

86

87 The neural correlates of embodied simulation during perspective-taking were recently

88 investigated by Wang et al. (2016) using Magnetoencephalography (MEG, Expt. 1) and

89 converging effects were found in the right posterior temporo-parietal junction (pTPJ) for

90 cognitive effort of perspective-taking (amount of angular disparity between self vs. other's

91 viewpoint) and for embodied processing (posture congruence) during perspective-taking (but

92 not for tracking). The crucial role of right pTPJ for perspective-taking was further confirmed

93 via transcranial magnetic stimulation (TMS) interference (Wang et al. 2016). The authors

94 further reported that low frequency theta oscillations (3-7 Hz) were the prominent neural

95   code in pTPJ, whilst Gooding-Williams et al. (2017) used repetitive TMS entrainment over

96   pTPJ to show that TMS pulses administered at theta frequency (6Hz) accelerated perspective-

97   taking, while alpha (10Hz) entrainment slowed perspective-taking down. TPJ-theta could

98   therefore be the relevant neural frequency to enable phase-coupling within a wider

99   mentalizing network.

100

101   These results build upon a perspective-taking EEG study which found an evoked component

102   at 450ms, localised primarily to the right TPJ (McCleery et al. 2011). Furthermore, they are

103   consistent with the neural correlates of perspective-taking reported using fMRI – two meta-

104   analyses (Van Overwalle 2009, 2011) have suggested that the core areas of activation include

105   bilateral TPJ and ventro-medial pre-frontal cortex (vmPFC). The posterior division of the TPJ

106   (Igelström and Graziano 2014; Bzdok et al. 2013) in particular, has been reliably linked to

107   perspective-taking and more generally to "mentalizing" (representing other's mental states)

108   (Van Overwalle 2011; Schurz et al. 2013), as well as to so-called spontaneous "out-of-body

109   experiences" (OBE) (Blanke et al. 2005). During an OBE individuals experience the

110   sensation that the self has moved to a different physical location than their body, and this

111   sensation often entails a translation as well as a rotation of perspective, similar to a deliberate

112   perspective transformation during perspective-taking (Kessler and Braithwaite 2016). The

113   involvement of TPJ in OBEs (Blanke et al. 2005) is of importance, as it corroborates the

114   proposed link between embodied processing and high-level social mentalizing in TPJ (Blanke

115   et al. 2005; Lombardo et al. 2010; Kessler and Braithwaite 2016; Wang et al. 2016).

116

117   Whilst the TPJ is clearly important for embodied processing and perspective-taking, the

118   region is also implicated in a range of cognitive operations, including spatial attention, social

119   cognition and self/other distinctions. It has been suggested that more generally, the region

6

120 acts as a major hub for information integration (Igelström and Graziano 2017.; Eddy 2016),

121 especially during higher-level cognitive processes relying upon internal representations, such

122 as perspective-taking (Igelström and Graziano 2017.; Eddy 2016; Wang et al. 2016;

123 Gooding-Williams et al. 2017). Indeed, the TPJ has extensive functional connectivity to

124 many networks of the brain, including the fronto-parietal control (Vincent et al. 2008),

125 default mode (Mars et al. 2012), and ventral attention networks (Bzdok et al. 2013). We

126 therefore hypothesised that the TPJ contributes to the process of embodied transformation

127 through changes in patterns of whole-brain functional connectivity, via theta-band synchrony,

128 as would be predicted from the region's role as a network hub (Igelström and Graziano

129 2017.; Carter and Huettel 2013; Eddy 2016). However, investigations of perspective-taking

130 using connectivity analysis, e.g. in form of frequency-specific phase-coupling, are scarce. To

131 our knowledge, only one study to date (Bögels et al. 2015) has reported enhanced theta

132 phase-coherence between right TPJ and ventromedial prefrontal cortex (vmPFC) in a

133 condition that required participants to imagine another's visual experience. The major aim of

134 the current study was therefore to consolidate the crucial role of pTPJ theta oscillations in

135 perspective-taking by means of advanced network analyses.

136

137 In addition to the TPJ, Wang et al., reported increases in theta-band power for the lateral PFC

138 during the cognitive effort of perspective-taking (Wang et al. 2016). Activity within this

139 region during social cognition has been argued to reflect high-level reasoning and working

140 memory processes recruited more generally during complex perspective-taking and

141 mentalizing tasks (Van Overwalle 2011). However, there is emerging evidence that frontal

142 activity in lateral PFC but also in the anterior cingulate cortex (ACC) could play a more

143 nuanced role in perspective-taking by managing the conflict between self and other

144 perspectives (Samson et al. 2005; Bögels et al. 2015; Hartwright et al. 2015). For example

7

145 (McCleery et al. 2011) found late a (0.8-1.0s) frontal evoked response during perspective-

146 taking dependent on whether self perspective was consistent with an avatar's perspective . In

147 terms of theta-oscillations, this could potentially manifest as a direct connection between

148 lateral PFC and the core mentalizing network (Bögels et al. 2015) in TPJ and vmPFC (Van

149 Overwalle 2009, 2011). We were therefore interested in whether the TPJ becomes

150 functionally connected to various frontal and midline regions during perspective-taking

151 (Hartwright et al. 2015), and crucially determining the direction of this connectivity.

152

153 In conclusion, we set out to consolidate previous findings regarding the crucial role of TPJ

154 theta oscillations for generating the abstract social representations required for perspective-

155 taking (Bögels et al. 2015; Wang et al. 2016; Gooding-Williams et al. 2017), while

156 unravelling in detail the involved functional network in terms of dynamic oscillatory

157 coupling between brain areas, using MEG. Based on the considerations above, we expected

158 TPJ and (v)mPFC to form a mentalizing network synchronised via theta oscillations, related

159 to generating the abstract representation of another's perspective, while activation in parietal

160 body-schema areas and sensorimotor cortex would reflect the required embodied

161 transformation to generate this representation via rotation of the egocentric perspective

162 (Kessler and Rutherford 2010; Kessler and Thomson 2010; Surtees et al. 2013). In addition,

163 pACC and lPFC might play key roles in top-down executive control of the underlying

164 embodied transformation and in managing the conflict between physical self and transformed

165 self at the representational level.

166

167 **Materials and Methods**

168

169 *Participants*

170   Data were collected from 18 participants (4 male, 14 female, mean age = 27.55, SD = 5.86).

171   All participants had normal or corrected to normal vision and no history of neurological or

172   psychiatric illness. All experimental procedures complied with the Declaration of Helsinki

173   and were approved by the Aston University, Department of Life & Health Sciences ethics

174   committee. Written consent was obtained from all participants.

175

176   *Experimental Paradigm and Design*

177   The paradigm was adopted from a behavioural study by Kessler and Rutherford (2010). The

178   stimuli were coloured photographs (resolution of 1024×768 pixels), showing an avatar

179   seated at a round table shown from one of four possible angular disparities (see Fig. 1, left:

180   60°, 160° clockwise and anticlockwise). In each trial one of the grey spheres on the table

181   turned red indicating this sphere as the target. From the avatar's viewpoint, the target could be

182   either visible or occluded (VO) by a centrally resented black screen; or to the left or to the

183   right (LR) inducing perspective-tracking or perspective-taking, respectively. Stimuli were

184   presented in 12 mini-blocks of 32 trials, alternating between LR and VO conditions. On each

185   trial participants were asked to make a target location judgement according to the avatar's

186   perspective by pressing the instructed key on an MEG-compatible response pad: the left key

187   for "left" or "visible" targets from the avatar's viewpoint and the right key for "right" or

188   "occluded" targets. Accuracy feedback was provided after each trial in the form of a short

189   tone. As in Kessler and Rutherford (2010), we collapsed across clockwise and anticlockwise

190   disparities, and separately collapsed correct responses for left and right and visible and

191   occluded, respectively. This resulted in four separate experimental conditions (for two

192   examples see Fig. 1, left): left/right judgements where the avatar is 160^0 from own

193   perspective (LR-160); left-/right judgements where the avatar is 60^0 from own perspective

194   (LR-60); visible/occluded judgments where the avatar is 160^0 from own perspective (VO-

9

195 160); visible/occluded judgments where the avatar is 60^0 from own perspective (VO-60).

196 This 2x2 design allowed us to disentangle perspective-taking from perspective-tracking and

197 investigate the effect of an increased angle of disparity (we chose to use 160° vs. 60° based

198 on the results of Wang et al., 2016), between self-perspective and other-perspective, which

199 has been shown to lengthen reaction times during perspective-taking (Kessler and Rutherford

200 2010; Surtees et al. 2013).

201

202 *Behavioural Data Analysis*

203 Behavioural reaction times (RT) from the experimental paradigm were extracted from E-

204 Prime® data files and converted to *.csv* format. Data from two participants with MEG

205 movement over 5mm was discarded. All trials containing incorrect answers or response times

206 greater than 2 standard deviations from the median were excluded from subsequent analyses.

207 For the four experimental conditions (LR-160; LR-60; VO-160; VO-60), median RT from

208 each participant were entered into a one-way ANOVA using the JASP statistics package.

209

210 *MEG and Structural MRI Acquisition*

211 MEG data were acquired using a 306-channel Neuromag MEG scanner (Vectorview, Elekta,

212 Finland) made up of 102 triplets of two orthogonal planar gradiometers and one

213 magnetometer. All recordings were performed inside a magnetically shielded room at a

214 sampling rate of 1000Hz. Five head position indicator (HPI) coils were applied for

215 continuous head position tracking, and visualised post-acquisition using an in-house Matlab

216 script. Two participants had excessive head movement (>5mm), and were excluded from

217 subsequent analyses. For MEG-MRI coregistration purposes three fiducial points, the

218 locations of the HPI coils and 300-500 points from the head surface were acquired using the

219 integrated Polhemus Fastrak digitizer. Visual stimuli were presented on a projection screen

10

220   located 86cm from participants, and auditory feedback through MEG-compatible

221   headphones. Data acquisition was broken down into three sequential runs, each lasting 8-10

222   minutes.

223

224   A structural T1 brain scan was acquired for source reconstruction using a Siemens

225   MAGNETOM Trio 3T scanner with a 32-channel head coil (TE=2.18ms, TR=2300ms,

226   TI=1100ms, flip angle=9°, 192 or 208 slices depending on head size, voxel-size =

227   0.8x0.8x0.8cm).

228

229   *MEG Preprocessing*

230   All MEG data were pre-processed using Maxfilter (temporal signal space separation, .96

231   correlation), which supresses external sources of noise from outside the head (Taulu and

232   Simola 2006). To compensate for head movement between runs, data from runs 2 and 3 were

233   transformed to participant's head position at the start of the first block using the *–trans* option

234   of Maxfilter. For each participant, the entire recording was band-pass filtered between 0.5-

235   250Hz (Butterworth filter) and band-stop filtered to remove residual 50Hz power-line

236   contamination and its harmonics. Data were then epoched into segments of 2500ms (1000ms

237   pre, 1500post stimulus onset) and each trial was demeaned and detrended. Trials containing

238   artefacts (SQUID jumps, eye-blinks, head movement) were removed by visual inspection,

239   resulting in removal of an average of 6.14% of trials per condition, per participant (additional

240   descriptive statistics reported in Table S1). For sensor-level analyses, ICA was used to

241   identify and reduce residual EOG and ECG artefacts. Four MEG channels containing large

242   amounts of non-physiological noise were removed from all source-level analyses. The pre-

243   processed data were then separated into the four experimental conditions and downsampled

244   to 250Hz to aid computation time.

245

246 *MEG-MRI Coregistration*

247 MEG data were co-registered with participants' T1 MRI structural scan by matching the

248 digitised head shape data with surface data from the structural scan (Jenkinson and Smith

249 2001). Subsequently, the aligned MRI-MEG image was used to create (i) a forward model

250 based on a single-shell description of the inner surface of the skull (Nolte 2003), using the

251 segmentation function in SPM8 and (ii) spatial normalisation parameters to create individual

252 volumetric grids. To facilitate group analysis, each individual volumetric grid was warped to

253 a template based on the MNI brain (8mm resolution). Subsequently the inverse of the

254 normalisation parameters were applied to the template grid, for source analysis.

255

256 *Sensor Level Analysis*

257 Sensor-level time-frequency representations (TFRs) were calculated using a single Hanning

258 taper between frequencies of 1-30Hz in steps of 1Hz. The entire 2500ms epoch was used,

259 with a sliding window of 500ms, but the first 250ms and last 500ms of each trial were

260 discarded to avoid edge artefacts. Due to different scales between the two MEG sensor-types,

261 only data from the gradiometers were used, with TFR power averaged across each pair post-

262 hoc. All analyses were computed on single trials and subsequently averaged, and therefore

263 TFRs contain both phase-locked (evoked) and non phase-locked (induced) information. As

264 hypothesised from previous research using a similar paradigm (Wang et al. 2016), TFR

265 responses averaged across subjects showed prominent differences between conditions within

266 the theta-band (2-7Hz).

267

268 For statistical testing, we therefore compared theta-band (2-7Hz), alpha (8-12Hz) and beta

269 (13-30Hz) power during trials in which the avatar was 160^0 versus 60^0 from the participant's

12

270 own perspective (clockwise or anticlockwise), in both left/right judgements (i.e. perspective-

271 taking), and visible/occluded judgements (i.e. perspective-tracking). We corrected for

272 multiple comparisons across time, frequency and space via cluster-based non-parametric

273 permutation testing (Maris and Oostenveld 2007). Results showed a significant cluster of

274 greater (3-6Hz) theta-band power at 0-650ms in the LR-160 versus LR-60 condition

275 (highlighted in Fig S1, left), but not for VO-160 vs. VO-60, (Fig. S1, right).

276

277 *MEG Source-Level*

278 Source localisation was conducted using Dynamical Imaging of Coherent Sources (Gross et

279 al. 2001) (DICS) which applies a spatial filter to the MEG data at every voxel of a canonical

280 0.8 cm brain-grid, in order to maximise signal from that location whilst attenuating signals

281 elsewhere. The spatial filter was calculated from the cross-spectral densities for a time–

282 frequency tile centred on the effects found at sensor level (3-6Hz; 0–650ms; gradiometer

283 channels only; see Fig. 1, top-right; Supplementary Figure S1). For all analyses, a common

284 filter across baseline and active periods was used and a regularisation parameter of lambda

285 5% was applied. Cluster-based non-parametric permutation testing was used to correct for

286 multiple comparisons across voxels (Maris and Oostenveld 2007), for the LR-160>LR-60

287 and VO-160>VO-60 contrasts. The resulting whole-brain statistical maps were spatially

288 smoothed using a robust smoothing algorithm (Garcia 2010) as implemented in bspmview,

289 and presented on a 3D cortical mesh using the Connectome Workbench software (Van Essen

290 et al. 2012). Using the spatial filters computed during source analysis, we extracted trial-by-

291 trial time-courses from three regions of interest, as shown in Fig. 2A, using the MNI co-

292 ordinates with the highest t-value within each region (Table S3).

293

294 *Granger Causality Analysis*

295 The directed functional connectivity between these three ROIs was estimated using

296 spectrally-resolved non-parametric Granger causality (Dhamala et al. 2008) as implemented

297 in the Fieldtrip toolbox (Oostenveld et al. 2010). Intact and scrambled time-series were split

298 into 0.325s epochs to enhance the accuracy of the results (0-0.65s post stimulus onset),

299 followed by Fourier transformation (Hanning taper; 2Hz spectral smoothing), before being

300 entered into a non-parametric spectral matrix factorisation procedure. Granger causality was

301 then estimated between each ROI pair and each ROI-scrambled time-series. Statistical

302 analysis was performed using cluster-based permutation testing (Maris and Oostenveld

303 2007). Granger causal influence between two regions (A & B) was deemed significant if

304 values were i) significantly greater than scrambled data (p<.05) and ii) significantly greater in

305 one direction than another (i.e. A-to-B versus B-to-A, p<.05).

306

307 *Theta-band Imaginary Coherence*

308 To estimate patterns of whole-brain connectivity supporting high-level perspective taking,

309 mediated by the right TPJ, we quantified theta-band phase synchrony during LR-160 trials

310 compared with LR-60 trials. A complex-valued spectral estimate at 5 ± 2Hz for each grid-

311 point was estimated using an adaptive spatial filter [the 'PCC' method, as implemented in

312 *ft_sourceanalysis* (Oostenveld et al. 2010)]. Coherence was used to quantify the phase

313 consistency between a seed region in TPJ (MNI co-ordinates [40 -58 36]) and every other

314 voxel of the canonical 0.8 cm brain-grid, using *ft_connectivityanalysis* (Oostenveld et al.

315 2010). Coherence values are normalised to range from 0 (no phase synchrony) to 1

316 (completely phase synchronised). We opted to project the complex-valued coherency

317 estimates onto the imaginary axis, as suggested by Nolte et al., (Nolte et al. 2004). This

318 removes estimates of instantaneous phase, thereby reducing the influence of spurious

319 connectivity resulting from MEG field spread (Nolte et al. 2004), but comes at the expense of

14

320   removing genuine connectivity at zero-lag. Further details on the quantification of

321   "imaginary coherence" can be found elsewhere (Nolte et al. 2004; Oostenveld et al. 2010).

322   Whole-brain coherence maps from LR-160 and LR-60 trials were baseline-corrected and

323   compared using cluster-based permutation-testing as implemented in the Fieldtrip toolbox

324   (Oostenveld et al. 2010). The resulting whole-brain statistical maps were spatially smoothed

325   using a robust smoothing algorithm (Garcia 2010) as implemented in bspmview, and

326   presented on a 3D cortical mesh using the Connectome Workbench software (Van Essen et

327   al. 2012).

328

329   *Supplementary Methods and Analysis Code*

330   Additional details are provided in SI Materials and Methods. MATLAB code for all analyses

331   is openly available online at

332   https://github.com/neurofractal/perspective_taking_oscillatory_networks (Seymour 2017).

333

334   **Results**

335

336   *Behavioural Results*

337   For the four experimental conditions, median reaction times (RT) from each participant were

338   entered into a one-way ANOVA (output detailed in Table S2). Results showed a main effect

339   of experimental condition on RT, $F(3,60) = 4.43$, p=.007, $\eta^2 = 0.181$. Post-hoc tests revealed

340   this was due to significantly longer RT for the LR-160 conditions compared with all other

341   conditions (LR-60, p_{tukey}= .013; VO-160, p_{tukey}= .029; VO-60, p_{tukey}= .026), replicating

342   Kessler and Rutherford (2010). The raw statistical output is reported in Table S2.

343
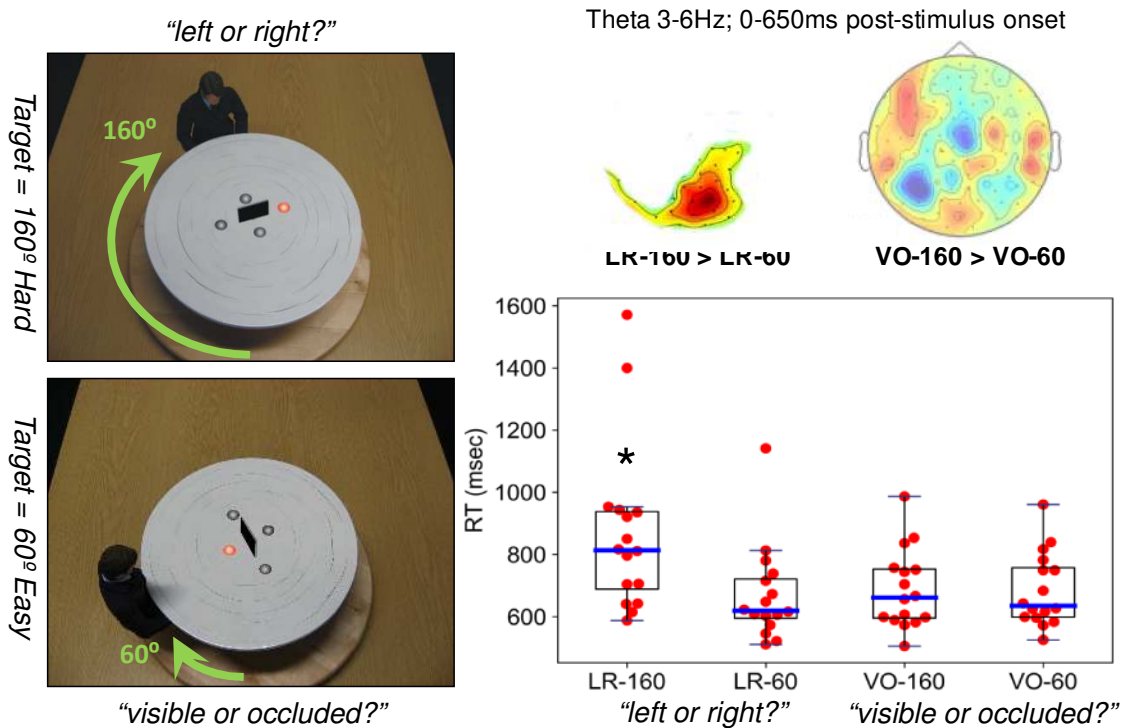
Figure 1. Left: Experimental paradigm (Kessler and Rutherford 2010) showing two example

stimuli (see Materials and Methods for details). Bottom right: Boxplot of participants' (N =

16, 2 participants removed with excess head movement) median reaction time (RT) in

milliseconds for the two angular disparity conditions (160 vs. 60) of perspective-taking (L/R)

and perspective-tracking (V/O), respectively. * = LR-160 is significantly different from all

other conditions (p<.05). Top right: Sensor-level topoplots of theta activity (3-6Hz), showing

a significant cluster (high visibility) for perspective-taking but not for perspective-tracking

(further details in Materials and Methods and supplementary information).

Task-Related Changes in Theta Power

Using a data-driven approach from 2-30Hz, time-frequency results at the sensor-level (see

Fig. 1 and Fig. S1) replicated the crucial role of theta oscillations in perspective-taking

(Wang et al. 2016; Gooding-Williams et al. 2017). A significant positive cluster (p=0.03) was

found at 3-6Hz, 0-650ms, when comparing angular disparities of 160° and 60° degrees for

359   the L/R task. No significant effects were found for any other frequencies (p>.05). In addition,

360   no significant clusters were found for the V/O task, i.e. perspective-tracking in the VO-160 vs

361   VO-60 contrast.

362

363   [Inline supplementary material - Insert Figure S1 here]

364

365   Based on these sensor-level data, which replicate our previous study (Wang et al., 2016), we

366   decided to concentrate on further characterising theta-band power and connectivity

367   underlying perspective-taking. Whilst a wider frequency range, that also included higher

368   delta frequencies, has been used to define theta-band power in previous studies (Wang et al.

369   2016), we opted to use 3-6Hz, based on the statistical analysis of the sensor-level data in

370   order to achieve the best signal-to-noise ratio for subsequent beamforming analyses.

371

372   To investigate the cortical sources underlying this effect of angular disparity, theta-band (3-

373   6Hz) power was localised from 0-650ms post-stimulus onset separately for 160° and 60°

374   trials, using the Dynamic Imaging of Coherent Sources (DICS) approach (see Materials and

375   Methods). Baseline-corrected theta (3-6Hz) power was compared for LR-160 versus LR-60

376   trials and VO-160 versus VO-60 trials across a 0.8cm cortical grid (Fig. 2A; Supplementary

377   Table S3). Results showed a significant (Maris and Oostenveld 2007) (p<.05) increase in

378   theta power during LR-160 trials compared with LR-60 trials for right posterior temporo-

379   parietal junction (pTPJ) spreading into the inter-parietal sulcus (IPS), for right lateral pre-

380   frontal cortex (PFC) primarily overlapping with the inferior frontal gyrus (IFG) and for right

381   anterior cingulate cortex (ACC). There was also a decrease in theta power in the LR-160

382   versus LR-60 condition in the left frontal pole (Table S3).

383

384 For perspective-tracking (VO-task), there were increases in theta-power, compared with pre-

385 trial baseline, within ventral occipital and temporo-parietal regions (Fig. S2). However, the

386 VO-160 > VO-60 contrast showed no significant clusters (Fig. S3), indicating that angular

387 disparity (160° versus 60°) only resulted in task-related increases in theta-band power for

388 high-level perspective-taking and not for perspective-tracking.

389
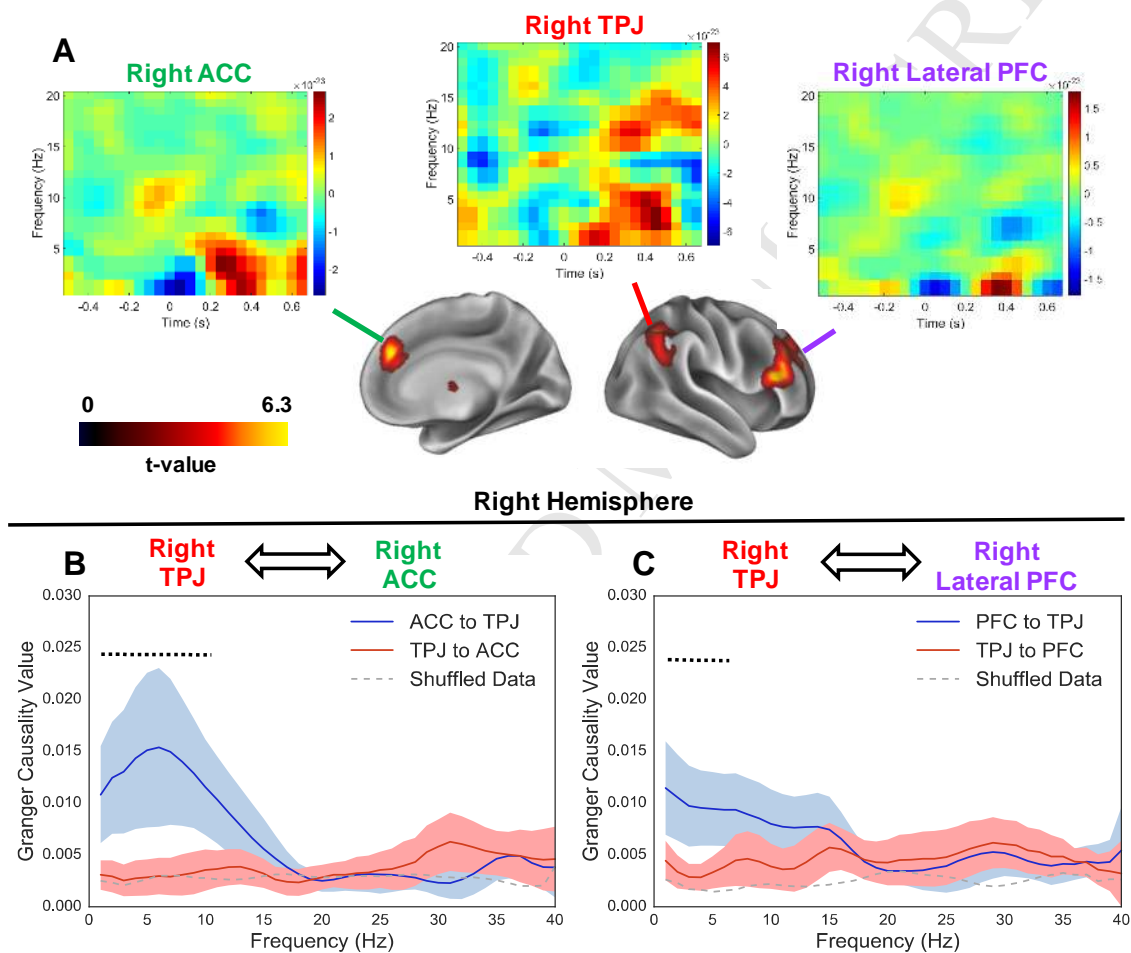
390

391 *Figure 2:* Theta power sources and directed connectivity. Panel A depicts brain plots

392 showing statistical results (clusters with p<.05 are shown) of a whole-brain DICS theta power

393 (3-6Hz) analysis for LR-160 > LR-60 contrast visualised using the Connectome Workbench

394 software (Van Essen et al. 2012) (see Table S3 for a complete list of power sources). Plots at

395 the top show time-frequency representations (LR-160 > LR-60 contrast) for three virtual

396 electrodes (VE) placed in right ACC (MNI co-ordinates: [12, 36, 28]), right TPJ (MNI co-

397 ordinates [40 -58 36]) and right lateral PFC (MNI co-ordinates: [52,32,16]). Panel B shows

398 spectrally resolved non-parametric Granger causality (1-40Hz), computed between the right

399 TPJ and (A) right ACC and (B) right lateral PFC, respectively. Results show an increase in

400 Granger causality from both the right ACC (1-10Hz) and right PFC (1-5Hz) to the right TPJ.

401 Shaded regions around each line represent 95% confidence intervals. The black dotted line

402 above the plots represents Granger causality values passing a p<.05 threshold (see Methods

403 for details). The grey dotted line in the plots shows shuffled data for comparison. Further

404 explanations in the text.

405

406   [Inline supplementary material - insert Figures S2 and S3 here]

407

408 *Virtual Electrode Time-Frequency Analysis*

409 To further investigate the oscillatory signatures of high-level perspective-taking, time-courses

410 for each trial were extracted from 'virtual-electrodes' in right TPJ, right ACC and right lateral

411 PFC (see Materials & Methods for details). Low-frequency oscillatory power was then

412 estimated between -0.65 to 0.65s post-stimulus using a Hanning taper, 0.05s sliding window.

413 Results show very early and sustained theta power (3-6Hz) increases in the right TPJ (0-0.5s)

414 for LR-160 versus LR-60 trials. Right lateral PFC delta/theta power (1-5Hz) and right ACC

415 (1-5Hz) increases are more transient and begin from 0.2-0.5s post-stimulus onset. This

416 suggests that the rTPJ is engaged throughout the process of embodied perspective-taking,

417 whereas increases in theta power ACC and PFC occur later and more transiently.

418

419 *Granger Causality Analysis*

19

420 To investigate directed functional connectivity during perspective-taking between the three

421 main regions of interest (ROIs) identified in the source power analysis (rTPJ, rACC and

422 rPFC), we employed spectrally resolved non-parametric Granger causality (GC) on LR trials

423 (0-0.65s post-stimulus onset) (Dhamala et al. 2008). GC is a statistical concept used to

424 estimate directed connectivity between time-series, which relies on the premise that if the

425 time-series of region *A* can be used to predicts the time-series of region *B*, then *A* is said to

426 'granger-cause' *B* (Ding Mingzhou et al. 2006). GC can also be extended to the frequency

427 domain (discussed further in (Bastos and Schoffelen 2016). Spectrally-resolved GC therefore

428 provides information about the direction of connectivity between regions of interest, as well

429 as the frequency-band underlying the effects.

430

431 Between the three ROIs, GC values showed statistically significant differences from fourier-

432 scrambled time-series in two pairs: rTPJ-rACC and rTPJ-rPFC (Maris and Oostenveld 2007).

433 To investigate these effects further, we statistically compared GC values between each

434 direction of the ROI pair (i.e. the granger causal influence to and from the rTPJ). Results

435 showed an asymmetric increase in granger causal influence, directed from right ACC

436 between 1-10Hz, with a peak at 6Hz, (Fig. 2B, p=.009) and right PFC, between 1-6Hz, (Fig

437 2B, p=.04) to the right TPJ.

438

439 *Imaginary Coherence*

440 Phase-synchronised neural activity has been argued to act as a mechanism for information

441 flow between brain regions during cognitive tasks (Womelsdorf et al. 2007). Measures of

442 phase synchrony (e.g. coherence) can therefore provide information about changes in brain

443 connectivity within a particular frequency band. However unlike GC, coherency alone does

444 not provide information about the direction of connectivity.

445

446   To establish patterns of whole-brain functional connectivity accompanying right-hemisphere

447   TPJ theta-band activity, we extracted source-level theta-band (5±2 Hz) phase relationships

448   from the sensor-level cross-spectral density matrix (see Materials and Methods). A measure

449   of phase synchrony between a right-TPJ seed and every other voxel was calculated by
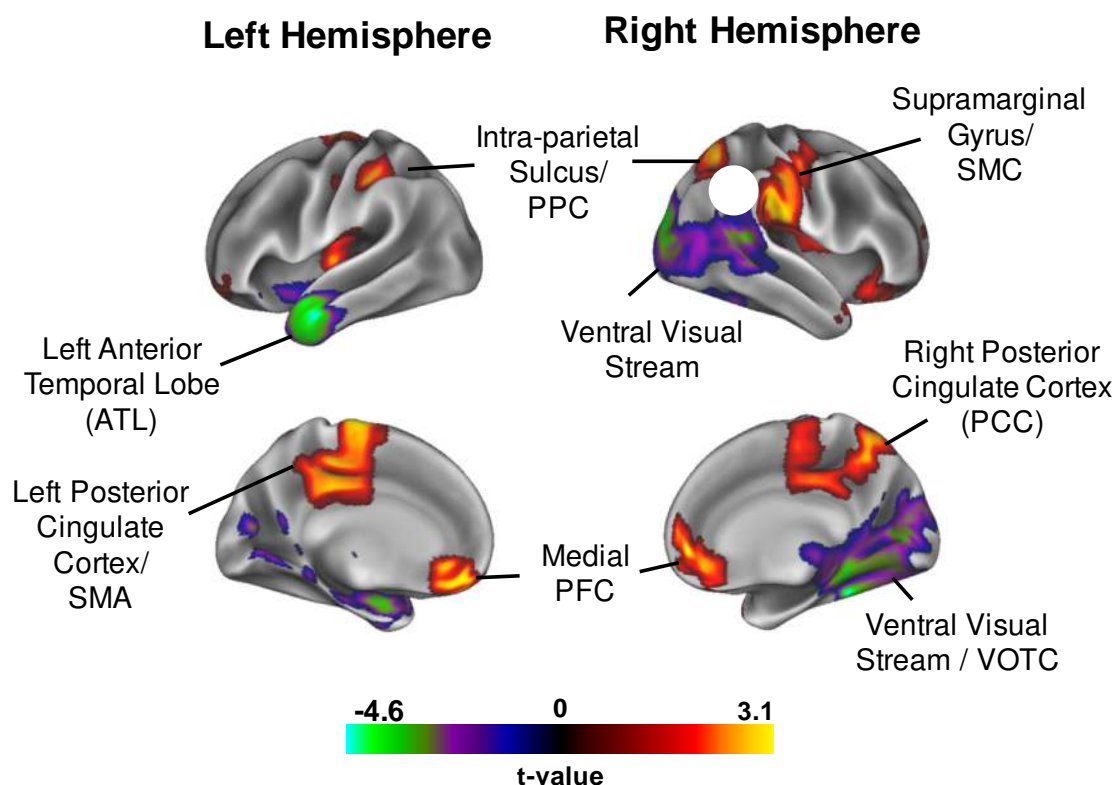
450   projecting complex-valued coherency onto the imaginary axis (Nolte et al. 2004). The

451   resulting coherency maps from the LR-160 and LR-60 conditions were first baseline-

452   corrected, and then compared using cluster-based non-parametric permutation testing (Maris

453   and Oostenveld 2007).

454

455

456   *Figure 3:* Results of a whole-brain imaginary coherence analysis in relation to a right TPJ

457   seed (white circle) and for a LR-160 > LR-60 contrast, visualised using the Connectome

458   Workbench software (Van Essen et al. 2012) (see Table S4 for a complete list of sources and

459 associated p-values). Clusters of coherency increase/decrease passing a p<.05 threshold are

460 shown (see Material and Methods). PPC = posterior parietal cortex; SMC = sensorimotor

461 cortex; SMA = supplementary motor area; PFC = prefrontal cortex; VOTC = ventral

462 occipitotemporal cortex.

463

464 Results (Fig. 3) show a complex pattern of both increased and decreased theta-band phase

465 synchrony during embodied perspective-taking. The main areas of decreased synchrony are

466 located in the ventral occipitotemporal cortex (VOTC), overlapping with key regions of the

467 ventral visual stream. There were also reductions in phase synchrony to the bilateral anterior

468 temporal lobes (ATL). Increased phase synchrony was observed in bilateral medial PFC

469 regions, posterior cingulate cortex (PCC), intra-parietal sulcus (IPS), supplementary motor

470 area (SMA), posterior parietal cortex (PPC), and right supramarginal gyrus/sensorimotor

471 cortex (SMC). These patterns of phase synchrony are unlikely to be driven by spurious

472 connectivity from MEG field spread (Brookes et al. 2011), as we opted to measure imaginary

473 coherence (Nolte et al. 2004), thereby removing effects in relation to instantaneous phase.

474

475

476 **Discussion**

477 This MEG study has investigated the oscillation-based functional connectivity between brain

478 regions involved in our ability to take another person's visuospatial perspective. Behavioural

479 results replicated a substantial body of research showing significantly increased reaction time

480 for higher angular disparity between the participant and avatar (160° versus 60°) for

481 perspective-taking but not perspective-*tracking* (Kessler and Rutherford 2010; Kessler and

482 Thomson 2010; Surtees et al. 2013; Wang et al. 2016). Greater angular disparity for

483 perspective-taking was accompanied by increased theta power (3-6Hz) within the right

484 TPJ/IPS and lateral PFC, replicating Wang et al., (Wang et al. 2016), as well as within the

485 right ACC. Importantly, this increase in theta-power for angular disparity was specific to

486 perspective-taking and not perspective-tracking (Figs. 1, S1, S3). We therefore focused on

487 network connectivity during perspective-taking and showed (Fig. 2) that there was an

488 increase in Granger causal influence (Dhamala et al. 2008) from lateral PFC and right ACC

489 *to* right TPJ, but not vice-versa, mediated by low frequency brain rhythms (1-10Hz). Finally,

490 we examined how whole-brain patterns of theta-band (5±2 Hz) phase synchrony, quantified

491 using imaginary coherence (Nolte et al. 2004), varied in relation to right TPJ activity. Results

492 (Fig. 3) suggest that with increasing angular disparity (160° versus 60°), the right TPJ

493 increases its phase coupling to regions involved in theory of mind (Carrington and Bailey

494 2009) (medial PFC, PCC) and body schema (Coslett et al. 2008; Medina et al. 2009) (SMC,

495 PPC, SMA), but decreases its phase coupling to visual regions (VOTC) and to bilateral

496 anterior temporal lobe (ATL). Overall, these results suggest a crucial role for TPJ as a hub

497 that functionally connects mentalizing, executive, and body-representational networks via

498 theta-band (3-7Hz) oscillations during high-level perspective taking (Fig. 4).

499

500 *The role of the right TPJ in high-level perspective-taking*

501 Results from this study suggest that the right TPJ (rTPJ) becomes increasingly engaged with

502 the need for embodied mental alignment during perspective-taking i.e. as the disparity grows

503 between our own and other's perspectives (Wang et al. 2016; Gooding-Williams et al. 2017).

504 Activity within the right TPJ is consistent with its role in establishing a sense of self (Blanke

505 et al. 2005), and crucially in differentiating conflicts between the self and other (Santiesteban

506 et al. 2012; Sowden and Catmur 2015; Eddy 2016). The left TPJ has also been implicated in

507 theory of mind and perspective-taking tasks (Santiesteban et al. 2012; Schurz et al. 2013),

508 however our results, replicating Wang et al., (2016) suggest that theta-band power is stronger

509 within the right TPJ, when there is a large angle of disparity (e.g. 160°) between self and

510 other perspective is greatest. This is consistent with some findings of lateralisation in TPJ

511 function (Igelström and Graziano 2017.). Given the importance of the rTPJ in perspective-

512 taking (Santiesteban et al. 2012; Schurz et al. 2015; Eddy 2016; Wang et al. 2016), we were

513 interested in further describing the neurocognitive processes involved.

514

515 As previous research has implicated the TPJ as a major network hub (Igelström and Graziano

516 2017.; Bzdok et al. 2013), we hypothesised that the region would co-ordinate shifts in

517 functional connectivity to other brain regions, via phase synchrony (Engel et al. 2001; Varela

518 et al. 2001). Indeed, we found that the rTPJ increased its phase-coupling to the medial PFC

519 and posterior PCC – two regions also involved more generally in understanding the mental

520 states of others (Lieberman 2007; Carrington and Bailey 2009; Van Overwalle 2009) (i.e.

521 mentalizing). Importantly, phase-coupling at theta frequency between rTPJ and medial PFC

522 had been previously reported by Bögels et al (2015) during a high-level mentalizing task.

523 Thus, TPJ-mPFC coupling could be part of a basic mechanism involved in simpler as well as

524 in more sophisticated forms of social mental alignment.

525

526 We also found increased phase synchrony between the rTPJ and SMC, SMA, and PPC (Fig.

527 3), regions previously implicated in coding for the body schema, i.e. cortical correlates of the

528 internal representation of the body and its postures and actions (Coslett et al. 2008; Medina et

529 al. 2009). We propose that this functional link, which has been reported previously (Arzy et

530 al. 2006; Cazzato et al. 2015), underlies the simulated rotation of the embodied self into

531 another's orientation and perspective, which so far has primarily been described

532 behaviourally (Kessler and Rutherford 2010; Surtees et al. 2013; Wang et al. 2016). The rTPJ

533 also showed decreased phase synchrony with visual regions (VOTC), primarily the ventral

534 stream of the right visual cortex, during high-level perspective-taking. Altogether, these

535 findings can be interpreted as an active shift from externally-driven processing (i.e. bottom-

536 up sensory information) to internal representations (i.e. self, body-schema rotation) during

537 high level perspective-taking. This switch from processing external events to updating

538 internal states and information has been previously linked with TPJ function (Bzdok et al.

539 2013; Wu et al. 2015).

540

541 Taken together, these findings suggest that rTPJ acts as a hub for high-level perspective

542 taking by routing visual information to internal representations of the self, the body and its

543 action and posture repertoire, via theta-band phase synchronisation (Figure 4). This allows

544 humans to actively project their own sense of self into another's viewpoint, resulting in rapid

545 and accurate perspective-taking responses (Kessler and Rutherford 2010; Surtees et al. 2013;

546 Wang et al. 2016; Gooding-Williams et al. 2017). However, given the simplicity of the

547 stimuli and required decisions (left or right) the social relevance of the current task and

548 associated processing could be called into question. Therefore, we would like to point out

549 that Kessler and Wang (2012) reported that social skills (social skills subscale of the AQ,

550 Baron-Cohen et al., 2001) and gender significantly predicted speed and embodiment of

551 responses on this task, suggesting that social abilities are linked to embodied perspective

552 taking even in this repetitive and simplified experimental form. Furthermore, using exactly

553 the same tasks, Kessler et al (2014,Proc R Soc B) showed that while the basic mechanisms

554 for perspective-taking and -tracking are essentially the same for Western and East-Asian

555 participants, there are subtle but significant culture-related differences in terms of self- vs.

556 other-centred biases that have been interpreted as cultural manifestations of differing social

557 norms (e.g. Markus and Kitayama, 1991; also Wu, Barr, Gann, & Keysar, 2013).Finally,

558 Bögels et al (2015) reported very similar theta oscillatory coupling between right TPJ and

559 mPFC during a more complex task of social perspective taking, where participants needed to

560 judge whether an interactor in a different room was presented with the same visual object or

561 not, based on their previous communication. This is a genuinely social task in the sense of

562 imagining another person's current visual experience with the aim to enable successful

563 communication. During this high-level social task right TPJ was phase-coherent with

564 vmPFC, thus confirming our claim that this coupling is part of the basic mechanism for

565 simpler as well as for more sophisticated forms of social mental alignment.

566

567 Interestingly, the other side of the coin of the described embodied perspective-taking process

568 tied to TPJ seems to be that aberrant activity in TPJ contributes to involuntary shifts in

569 perspective, as experienced in so-called "out-of–body" experiences (OBE) (Blanke et al.

570 2005; Kessler and Braithwaite 2016). This emerging framework is consistent with a recent

571 model arguing that the TPJ acts as a "nexus", hub, or convergence zone between different

572 cognitive domains including social cognition, attention and executive function (Carter and

573 Huettel 2013). Our results suggest that the TPJ plays an important role during complex

574 social-cognitive processes like perspective-taking, by co-ordinating the activity between

575 multiple brain regions and functional sub-networks into a coherent whole (Santiesteban et al.

576 2012; Carter and Huettel 2013; Bögels et al. 2015; Eddy 2016) (Fig. 4). We further propose

577 that theta oscillations could be the crucial network code for this integration process (Bögels et

578 al. 2015; Wang et al. 2016; Gooding-Williams et al. 2017).

579

580 *Top-down Executive Processes during high-level perspective-taking*

581 Along with the rTPJ, two additional regions showed significantly increased theta power with

582 increasing angular disparity during perspective-taking (Fig. 2A): the lateral PFC, primarily

583 overlapping with the right inferior frontal gyrus; and the right ACC. This theta-band activity

584 was found during a slightly later period than the rTPJ, from 0.2-0.5 post-stimulus onset,

585 suggesting that the ACC and lateral PFC contribute later to the process of perspective-taking.

586 Interestingly, we also found that these two regions displayed directed functional connectivity,

587 as measured by Granger causality, to the rTPJ, mediated by low frequency brain rhythms (1-

588 10Hz), indicative of top-down processing (Von Stein et al. 2000).

589

590 Activity within the ACC and lateral PFC is typically associated with cognitive control (Aron

591 et al. 2014) and conflict monitoring (Botvinick et al. 2004). However recent work has shown

592 the regions to be also implicated in a number of theory of mind studies (Vogeley et al. 2001;

593 Hartwright et al. 2012, 2015; Samson et al. 2015). Activity within this context has been

594 argued to reflect the detection (Amodio and Frith 2006; Lieberman 2007) (ACC) and

595 resolution (Samson et al. 2005; Hartwright et al. 2012) (lateral PFC) of conflict between self

596 and other perspectives (Hartwright et al. 2016a). We therefore propose (Fig. 4) that the

597 connectivity from rACC and rPFC to rTPJ, during later stages of perspective-taking, reflects

598 domain-general "top-down" executive control processes (Duncan and Owen 2000) required

599 for suppressing the self-perspective, in favour of taking the other's perspective (Samson et al.

600 2005; Van der Meer et al. 2011; Hartwright et al. 2015), and/or for controlling the conflict

601 between the physical self and the transformed self (the "other") (May 2004; Santiesteban et

602 al. 2012; Wang et al. 2016), allowing both representations to co-exist in the brain, similar to

603 the experience of an OBE, where the self is located in two places at once (Kessler and

604 Braithwaite 2016). Our results differ slightly from those reported in (McCleery et al. 2011),

605 but our interpretations are not fully at odds with McCleery et al's, who argue that the lateral

606 PFC selects between self/other perspectives, both computed in the rTPJ, depending on task

607 demands, thus, favouring our second interpretation (i.e., ACC and lateral PFC managing the

608 conflict between self and other perspectives that may coexist in TPJ). At this stage it remains

609   unknown what information content exactly is computed in which part of the brain. Differing

610   results could also be due to differences in the paradigms employed – unlike (McCleery et al.

611   2011), perspective-taking stimuli in this study required differing levels of embodied

612   simulation, potentially requiring different levels of conflict management between self and

613   other perspectives. In addition, this study focussed on earlier frontal theta-band oscillations

614   (0-0.65s) compared with the later evoked frontal responses (0.6-0.8s) reported in (McCleery

615   et al. 2011). It should also be noted that perspective-tracking could also involve similar

616   cognitive control processes. However, the experimental contrast between different angular

617   disparities (160° vs 60°) may have precluded our ability to detect this, as similar executive

618   control processes would be equally engaged in both conditions.

619

620   More generally, whilst the involvement of executive-control processes in perspective-taking

621   is based on substantial empirical research (Aron et al. 2014; Hartwright et al. 2016a), to avoid

622   reverse-inference, future work could vary executive demands during perspective-taking

623   (Bradford et al. 2015), in combination with brain stimulation (Wang et al. 2016) to establish

624   the causal role of the lateral PFC and rACC. For example, one study has shown that theta-

625   burst TMS to lateral PFC slowed reaction times during a false belief task requiring a

626   dissociation between self and other perspectives, after modelling the structural morphology

627   of lateral PFC and right TPJ (Hartwright et al. 2016b). In addition, the observation that our

628   effects in ACC and PFC were primarily related to theta oscillations, further corroborates the

629   notion of top-down control, since theta has previously been shown to reflect top-down

630   cognitive control processes involved in conflict monitoring (Botvinick et al. 2004) and error-

631   related responses (Trujillo and Allen 2007). Our complimentary finding that the ACC and

632   lateral PFC exerted top-down influence on the TPJ via low frequency rhythms (1-10Hz,

28

633 peaking in theta) is clearly consistent with ACC and PFC theta as a mechanism for cognitive

634 control.

635

636 *Limitations*

637 This article, building on our previous work (Bögels et al. 2015; Wang et al. 2016; Gooding-

638 Williams et al. 2017), has focussed on the role of theta-band power and connectivity

639 underlying perspective-taking. Whilst sensor-level analysis revealed only a single positive

640 cluster of activity from 3-6Hz, corroborating our previous results, inspection of Figure 2A

641 suggests that these effects might spread into delta and low alpha frequency ranges. This is

642 also observed for right TPJ (power) and lateral PFC which peaks in delta (1-3Hz) rather than

643 theta (3-6Hz) in power and Granger causality spectra (Fig. 2). This discrepancy may explain

644 the lack of phase synchrony, probed at 5±2 Hz rather than 1-3Hz, between the right TPJ and

645 lateral PFC reported using imaginary coherence. It is worth noting that the fine-grained

646 definition of frequency ranges is confounded by spectral smoothing applied during the

647 frequency decomposition process. Future work should therefore attempt to clarify whether

648 there might be additional independent or multiplexed oscillatory networks (e.g. Seymour et

649 al. 2017) at different frequency ranges, including those between delta/theta and gamma

650 (>30Hz) bands (Cao et al. 2018). Nevertheless, this article suggests that theta (3-6Hz)

651 appears to be the most dominant oscillatory frequency band (if not the only band), underlying

652 embodied perspective-taking.

653

654 *Conclusion*

655 This study examined the cortical networks involved in high-level mental alignment

656 (perspective taking), co-ordinated by theta-band oscillations. Low-frequency phase coupling

657 in the theta-band, has previously been shown to contribute to the co-ordination of long-range

29

658 neuronal interactions (von Stein and Sarnthein 2000; Mizuhara et al. 2004), through which

659 distributed neural assemblies become integrated into a coherent network (Varela et al. 2001).

660 Our finding that theta-band phase-coupling synchronises the right temporo-parietal junction

661 (rTPJ) to brain regions involved in theory of mind and regions coding for body schema

662 supports this view, and suggests that perspective taking, and potentially other social cognitive

663 processes, involve the co-ordination of spatially and functionally disperse brain regions via

664 theta-band phase synchrony (von Stein and Sarnthein 2000), further supported by low-

665 frequency top-down influences from executive control areas (Bögels et al. 2015).

666
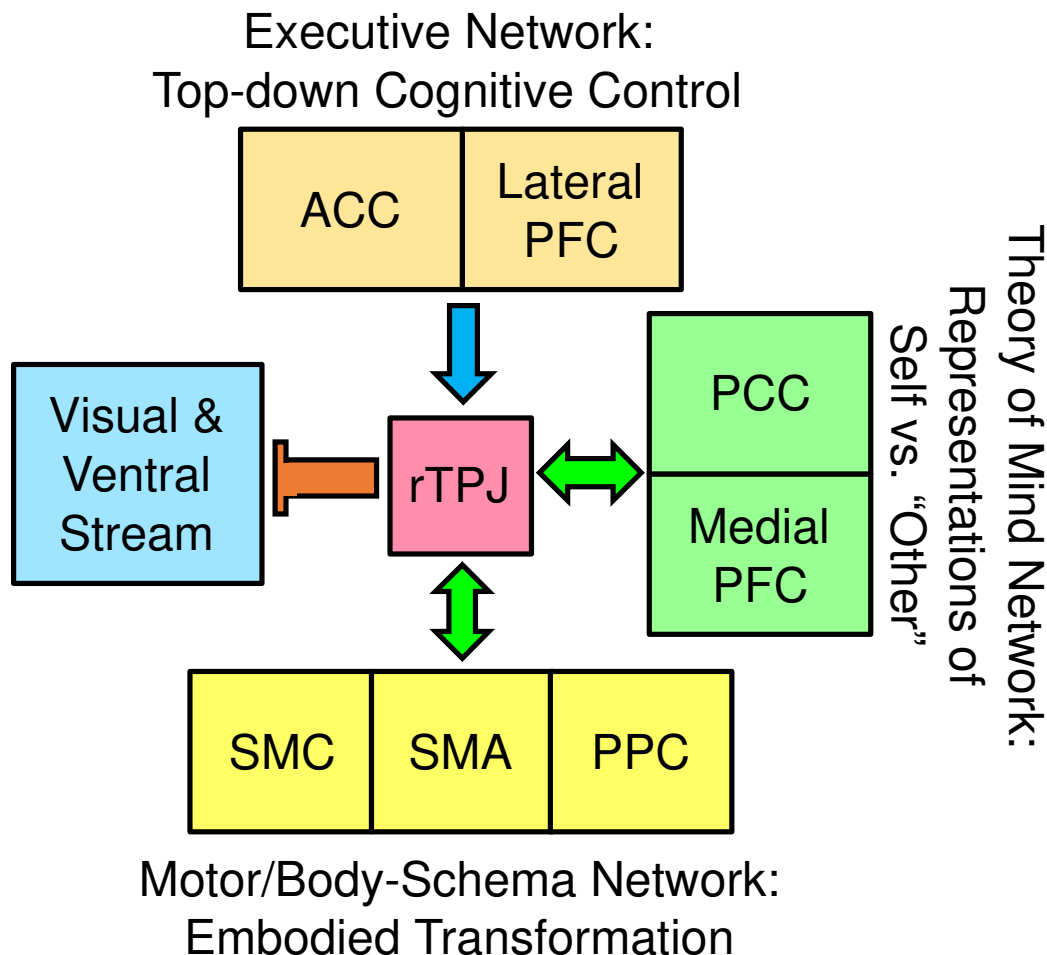
667

668 *Figure 4:* Proposed network underlying high-level perspective-taking (Kessler and

669 Rutherford 2010; Surtees et al. 2013), linked by power and phase in the theta-band (3-7Hz).

670   During initiation of embodied perspective-taking behaviour, early rTPJ activity co-ordinates

671   connectivity decreases with visual regions, whilst increasing connectivity with regions

672   involved in Theory of Mind, and Motor/Body-Schema. Increases in low frequency (primarily

673   theta) power within the lateral PFC and ACC reflect domain-general cognitive control

674   processes for detecting and managing top-down the conflict between self and other

675   perspectives.

676

681

682   **References:**

683   Amodio DM, Frith CD. 2006. Meeting of minds: the medial frontal cortex and social

684   cognition. Nat Rev Neurosci. 7:268.

685   Aron AR, Robbins TW, Poldrack RA. 2014. Inhibition and the right inferior frontal cortex:

686   one decade on. Trends Cogn Sci. 18:177–185.

687   Arzy S, Thut G, Mohr C, Michel CM, Blanke O. 2006. Neural Basis of Embodiment: Distinct

688   Contributions of Temporoparietal Junction and Extrastriate Body Area. J Neurosci.

689   26:8074–8081.

690   Baron-Cohen S, Wheelwright, S , Skinner R, Martin J, & Clubley, E. 2001. The autism-

691   spectrum quotient (AQ): Evidence from asperger syndrome/high-functioning autism,

692   malesand females, scientists and mathematicians. Journal of autism and

693   developmental disorders, 31:1, 5-17.

694   Bastos AM, Schoffelen J-M. 2016. A Tutorial Review of Functional Connectivity Analysis

695   Methods and Their Interpretational Pitfalls. Front Syst Neurosci. 175.

696   Blanke O, Mohr C, Michel CM, Pascual-Leone A, Brugger P, Seeck M, Landis T, Thut G.

697   2005. Linking out-of-body experience and self processing to mental own-body

698   imagery at the temporoparietal junction. J Neurosci. 25:550–557.

699   Bögels S, Barr DJ, Garrod S, Kessler K. 2015. Conversational interaction in the scanner:

700   mentalizing during language processing as revealed by MEG. Cereb Cortex. 25:3219–

701   3234.

702   Botvinick MM, Cohen JD, Carter CS. 2004. Conflict monitoring and anterior cingulate

703   cortex: an update. Trends Cogn Sci. 8:539–546.

704   Bradford EEF, Jentzsch I, Gomez J-C. 2015. From self to social cognition: Theory of Mind

705   mechanisms and their relation to Executive Functioning. Cognition. 138:21–34.

706   Bräuer J, Call J, Tomasello M. 2007. Chimpanzees really know what others can see in a

707   competitive situation. Anim Cogn. 10:439–448.

708   Brookes MJ, Hale JR, Zumer JM, Stevenson CM, Francis ST, Barnes GR, Owen JP, Morris

709   PG, Nagarajan SS. 2011. Measuring functional connectivity using MEG:

710   methodology and comparison with fcMRI. Neuroimage. 56:1082–1104.

711   Bugnyar T, Stöwe M, Heinrich B. 2004. Ravens, Corvus corax, follow gaze direction of

712   humans around obstacles. Proc R Soc Lond B Biol Sci. 271:1331–1336.

713   Bzdok D, Langner R, Schilbach L, Jakobs O, Roski C, Caspers S, Laird AR, Fox PT, Zilles

714   K, Eickhoff SB. 2013. Characterization of the temporo-parietal junction by combining

715   data-driven parcellation, complementary connectivity analyses, and functional

716   decoding. NeuroImage. 81:381–392.

717   Call J, Tomasello M. 1999. A nonverbal false belief task: The performance of children and

718   great apes. Child Dev. 70:381–395.

719 Cao W, Lin S, Xia Q, Du Y, Yang Q, Zhang M, Lu Y, Xu J, Duan S, Xia J, Feng G, Xu J,

720   Luo J. 2018. Gamma Oscillation Dysfunction in mPFC Leads to Social Deficits in

721   Neuroligin 3 R451C Knockin Mice. Neuron. 97:1253-1260.e7.

722 Carrington SJ, Bailey AJ. 2009. Are there theory of mind regions in the brain? A review of

723   the neuroimaging literature. Hum Brain Mapp. 30:2313–2335.

724 Carter RM, Huettel SA. 2013. A nexus model of the temporal–parietal junction. Trends Cogn

725   Sci. 17:328–336.

726 Cazzato V, Mian E, Serino A, Mele S, Urgesi C. 2015. Distinct contributions of extrastriate

727   body area and temporoparietal junction in perceiving one's own and others' body.

728   Cogn Affect Behav Neurosci. 15:211–228.

729 Coslett H, Buxbaum LJ, Schwoebel J. 2008. Accurate reaching after active but not passive

730   movements of the hand: Evidence for forward modeling. Behav Neurol. 19:117–125.

731 Dhamala M, Rangarajan G, Ding M. 2008. Analyzing information flow in brain networks

732   with nonparametric Granger causality. Neuroimage. 41:354–362.

733 Ding Mingzhou, Chen Yonghong, Bressler Steven L. 2006. Granger Causality: Basic Theory

734   and Application to Neuroscience. Handb Time Ser Anal, Wiley Online Books.

735 Duncan J, Owen AM. 2000. Common regions of the human frontal lobe recruited by diverse

736   cognitive demands. Trends Neurosci. 23:475–483.

737 Eddy CM. 2016. The junction between self and other? Temporo-parietal dysfunction in

738   neuropsychiatry. Neuropsychologia. 89:465–477.

739 Engel AK, Fries P, Singer W. 2001. Dynamic predictions: Oscillations and synchrony in top–

740   down processing. Nat Rev Neurosci. 2:704–716.

741 Flavell JH, Everett BA, Croft K, Flavell ER. 1981. Young children's knowledge about visual

742   perception: Further evidence for the Level 1–Level 2 distinction. Dev Psychol. 17:99.

743 Frith CD, Frith U. 2007. Social cognition in humans. Curr Biol. 17:R724–R732.

744 Garcia D. 2010. Robust smoothing of gridded data in one and higher dimensions with

745   missing values. Comput Stat Data Anal. 54:1167–1178.

746 Gooding-Williams G, Wang H, Kessler K. 2017. THETA-Rhythm Makes the World Go

747   Round: Dissociative Effects of TMS Theta Versus Alpha Entrainment of Right pTPJ

748   on Embodied Perspective Transformations. Brain Topogr. 1–4.

749 Gross s J, Kujala J, Hämäläinen M, Timmermann L, Schnitzler A, Salmelin R. 2001.

750   Dynamic imaging of coherent sources: studying neural interactions in the human

751   brain. Proc Natl Acad Sci. 98:694–699.

752 Gzesh SM, Surber CF. 1985. Visual perspective-taking skills in children. Child Dev. 1204–

753   1213.

754 Hartwright CE, Apperly IA, Hansen PC. 2012. Multiple roles for executive control in belief–

755   desire reasoning: Distinct neural networks are recruited for self perspective inhibition

756   and complexity of reasoning. NeuroImage. 61:921–930.

757 Hartwright CE, Apperly IA, Hansen PC. 2015. The special case of self-perspective inhibition

758   in mental, but not non-mental, representation. Neuropsychologia. 67:183–192.

759 Hartwright CE, Hansen PC, Apperly IA. 2016a. Current knowledge on the role of the Inferior

760   Frontal Gyrus in Theory of Mind – A commentary on Schurz and Tholen (2016).

761   Cortex. 85:133–136.

762 Hartwright Charlotte E., Hardwick Robert M., Apperly Ian A., Hansen Peter C. 2016b.

763   Resting state morphology predicts the effect of theta burst stimulation in false belief

764   reasoning. Hum Brain Mapp. 37:3502–3514.

765 Igelström KM, Graziano MSA. 2017. The inferior parietal lobule and temporoparietal

766   junction: A network perspective. Neuropsychologia.

767 Jenkinson M, Smith S. 2001. A global optimisation method for robust affine registration of

768   brain images. Med Image Anal. 5:143–156.

769   Kessler K, Braithwaite JJ. 2016. Deliberate and spontaneous sensations of disembodiment:

770   capacity or flaw? Cognit Neuropsychiatry. 21:412–428.

771   Kessler K, Cao L, O'Shea K J, Wang H. 2014. A cross-culture, cross-gender comparison of

772   perspective taking mechanisms. Proceedings of the Royal Society of London B:

773   Biological Sciences, 281:1785, 20140388.

774   Kessler K, Rutherford H. 2010. The Two Forms of Visuo-Spatial Perspective Taking are

775   Differently Embodied and Subserve Different Spatial Prepositions. Front Psychol.

776   1:213.

777   Kessler K, Thomson LA. 2010. The embodied nature of spatial perspective taking: embodied

778   transformation versus sensorimotor interference. Cognition. 114:72–88.

779   Kessler, K, Wang, H. 2012. Spatial perspective taking is an embodied process, but not for

780   everyone in the same way: differences predicted by sex and social skills score. Spatial

781   Cog & Comp, 12:2-3, 133-158.

782   Lieberman MD. 2007. Social cognitive neuroscience: a review of core processes. Annu Rev

783   Psychol. 58:259–289.

784   Lombardo MV, Chakrabarti B, Bullmore ET, Wheelwright SJ, Sadek SA, Suckling J, Baron-

785   Cohen S, Consortium MA, others. 2010. Shared neural circuits for mentalizing about

786   the self and others. J Cogn Neurosci. 22:1623–1635.

787   Maris E, Oostenveld R. 2007. Nonparametric statistical testing of EEG- and MEG-data. J

788   Neurosci Methods. 164:177–190.

789   Markus HR, Kitayama S. 1991. Culture and the self: Implications for cognition, emotion,

790   and motivation. Psychological review, 98:2, 224.

791   Mars RB, Sallet J, Schüffelgen U, Jbabdi S, Toni I, Rushworth MF. 2012. Connectivity-

792   based subdivisions of the human right "temporoparietal junction area": evidence for

793   different areas participating in different cortical networks. Cereb Cortex. 22:1894–

794   1903.

795   May M. 2004. Imaginal perspective switches in remembered environments: Transformation

796   versus interference accounts. Cognit Psychol. 48:163–206.

797   McCleery JP, Surtees ADR, Graham KA, Richards JE, Apperly IA. 2011. The Neural and

798   Cognitive Time Course of Theory of Mind. J Neurosci. 31:12849–12854.

799   Medina J, Jax SA, Coslett HB. 2009. Two-component models of reaching: Evidence from

800   deafferentation in a Fitts' law task. Neurosci Lett. 451:222–226.

801   Mizuhara H, Wang L-Q, Kobayashi K, Yamaguchi Y. 2004. A long-range cortical network

802   emerging with theta oscillation in a mental task. Neuroreport. 15:1233–1238.

803   Moll H, Tomasello M. 2006. Level 1 perspective-taking at 24 months of age. Br J Dev

804   Psychol. 24:603–613.

805   Nolte G. 2003. The magnetic lead field theorem in the quasi-static approximation and its use

806   for magnetoencephalography forward calculation in realistic volume conductors. Phys

807   Med Biol. 48:3637–3652.

808   Nolte G, Bai O, Wheaton L, Mari Z, Vorbach S, Hallett M. 2004. Identifying true brain

809   interaction from EEG data using the imaginary part of coherency. Clin Neurophysiol

810   Off J Int Fed Clin Neurophysiol. 115:2292–2307.

811   Oostenveld R, Fries P, Maris E, Schoffelen J-M. 2010. FieldTrip: open source software for

812   advanced analysis of MEG, EEG, and invasive electrophysiological data. Comput

813   Intell Neurosci. 2011.

814   Povinelli DJ, Bering JM, Giambrone S. 2000. Toward a science of other minds: Escaping the

815   argument by analogy. Cogn Sci. 24:509–541.

816   Samson D, Apperly IA, Kathirgamanathan U, Humphreys GW. 2005. Seeing it my way: a

817   case of a selective deficit in inhibiting self-perspective. Brain. 128:1102–1111.

818   Samson D, Houthuys S, Humphreys GW. 2015. Self-perspective inhibition deficits cannot be

819   explained by general executive control difficulties. Cortex. 70:189–201.

820   Santiesteban I, Banissy MJ, Catmur C, Bird G. 2012. Enhancing social ability by stimulating

821   right temporoparietal junction. Curr Biol. 22:2274–2277.

822   Schurz M, Aichhorn M, Martin A, Perner J. 2013. Common brain areas engaged in false

823   belief reasoning and visual perspective taking: a meta-analysis of functional brain

824   imaging studies. Front Hum Neurosci. 7.

825   Schurz M, Kronbichler M, Weissengruber S, Surtees A, Samson D, Perner J. 2015.

826   Clarifying the role of theory of mind areas during visual perspective taking: Issues of

827   spontaneity and domain-specificity. NeuroImage. 117:386–396.

828   Seymour RA. 2017. Neurofractal/perspective_taking_oscillatory_networks: Work in Progress

829   Release of Perspective Taking Data.

830   Seymour RA, Rippon G, Kessler K. 2017. The Detection of Phase Amplitude Coupling

831   during Sensory Processing. Front Neurosci. 11:487.

832   Sowden S, Catmur C. 2015. The role of the right temporoparietal junction in the control of

833   imitation. Cereb Cortex. 25:1107–1113.

834   Surtees A, Apperly I, Samson D. 2013. The use of embodied self-rotation for visual and

835   spatial perspective-taking. Front Hum Neurosci. 7.

836   Tomasello M, Carpenter M, Call J, Behne T, Moll H. 2005. Understanding and sharing

837   intentions: the origins of cultural cognition. Behav Brain Sci. 28:675–691; discussion

838   691-735.

839   Trujillo LT, Allen JJ. 2007. Theta EEG dynamics of the error-related negativity. Clin

840   Neurophysiol. 118:645–668.

841 Van der Meer L, Groenewold NA, Nolen WA, Pijnenborg M, Aleman A. 2011. Inhibit

842   yourself and understand the other: neural basis of distinct processes underlying

843   Theory of Mind. Neuroimage. 56:2364–2374.

844 Van Essen DC, Ugurbil K, Auerbach E, Barch D, Behrens TEJ, Bucholz R, Chang A, Chen

845   L, Corbetta M, Curtiss SW, others. 2012. The Human Connectome Project: a data

846   acquisition perspective. Neuroimage. 62:2222–2231.

847 Van Overwalle F. 2009. Social cognition and the brain: A meta-analysis. Hum Brain Mapp.

848   30:829–858.

849 Van Overwalle F. 2011. A dissociation between social mentalizing and general reasoning.

850   Neuroimage. 54:1589–1599.

851 Van Overwalle F, Baetens K. 2009. Understanding others' actions and goals by mirror and

852   mentalizing systems: a meta-analysis. Neuroimage. 48:564–584.

853 Varela F, Lachaux J-P, Rodriguez E, Martinerie J. 2001. The brainweb: phase

854   synchronization and large-scale integration. Nat Rev Neurosci. 2:229–239.

855 Vincent JL, Kahn I, Snyder AZ, Raichle ME, Buckner RL. 2008. Evidence for a

856   frontoparietal control system revealed by intrinsic functional connectivity. J

857   Neurophysiol. 100:3328–3342.

858 Vogeley K, Bussfeld P, Newen A, Herrmann S, Happé F, Falkai P, Maier W, Shah NJ, Fink

859   GR, Zilles K. 2001. Mind reading: neural mechanisms of theory of mind and self-

860   perspective. Neuroimage. 14:170–181.

861 Von Stein A, Chiang C, König P. 2000. Top-down processing mediated by interareal

862   synchronization. Proc Natl Acad Sci. 97:14748–14753.

863 von Stein A, Sarnthein J. 2000. Different frequencies for different scales of cortical

864   integration: from local gamma to long range alpha/theta synchronization. Int J

865   Psychophysiol. 38:301–313.

866   Wang H, Callaghan E, Gooding-Williams G, McAllister C, Kessler K. 2016. Rhythm makes

867   the world go round: An MEG-TMS study on the role of right TPJ theta oscillations in

868   embodied perspective taking. Cortex J Devoted Study Nerv Syst Behav. 75:68–81.

869   Womelsdorf T, Schoffelen J-M, Oostenveld R, Singer W, Desimone R, Engel AK, Fries P.

870   2007. Modulation of neuronal interactions through neuronal synchronization. Science.

871   316:1609–1612.

872   Wu S, Barr DJ, Gann TM, Keysar B. 2013. How culture influences perspective taking:

873   differences in correction, not integration. Frontiers in human neuroscience, 7, 822.

874   Wu Q, Chang C-F, Xi S, Huang I-W, Liu Z, Juan C-H, Wu Y, Fan J. 2015. A critical role of

875   temporoparietal junction in the integration of top-down and bottom-up attentional

876   control. Hum Brain Mapp. 36:4317–4333.

877   Zacks JM, Michelon P. 2005. Transformations of visuospatial images. Behav Cogn Neurosci

878   Rev. 4:96–118.

879

"left or right?"

Target = 160° Hard

160°

Target = 60° Easy

60°
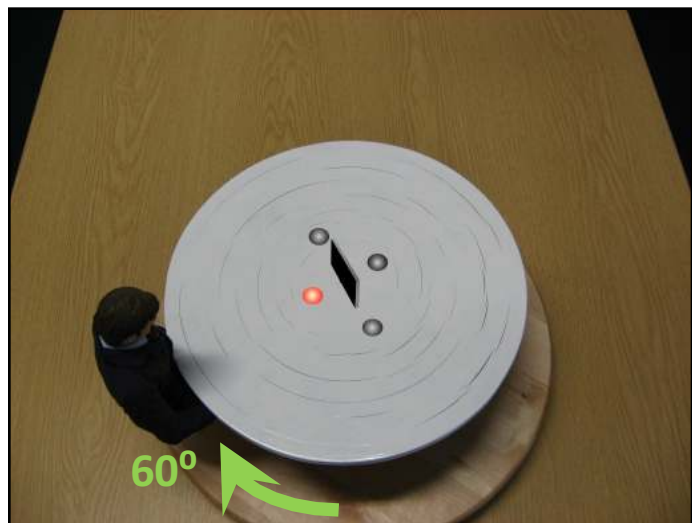
"visible or occluded?"

Theta 3-6Hz; 0-650ms post-stimulus onset

LR-160 > LR-60　　　**VO-160 > VO-60**

RT (msec)

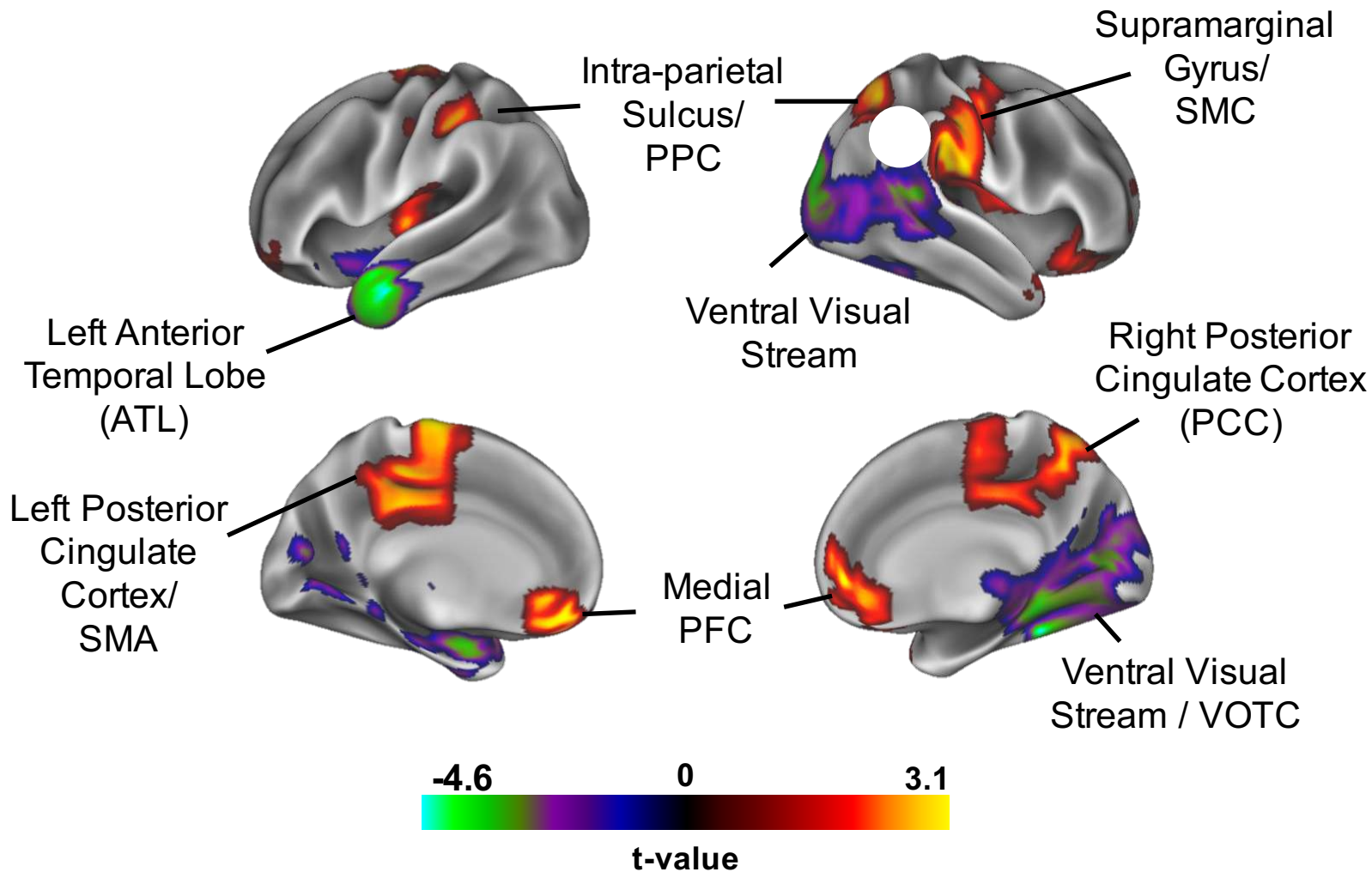*
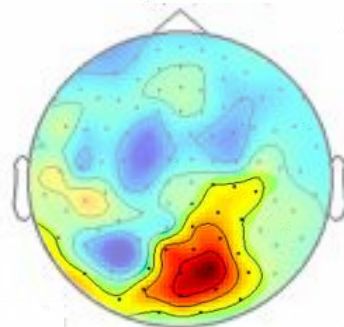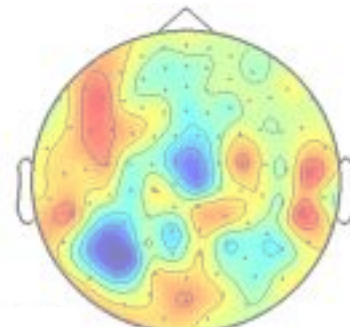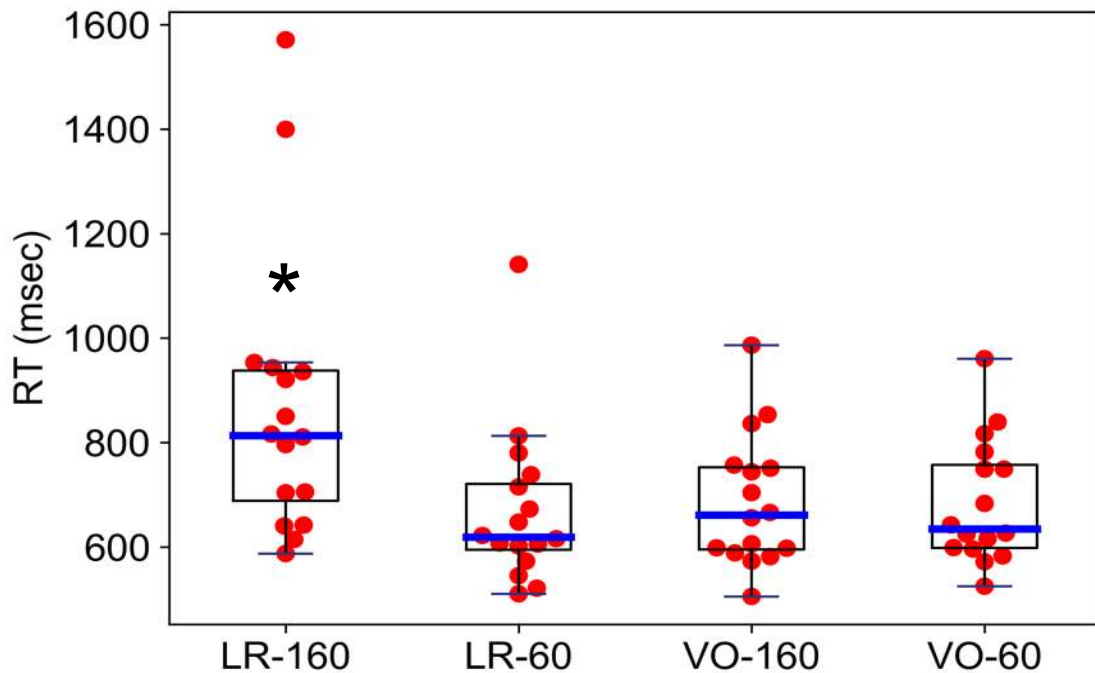
"left or right?"　　　*"visible or occluded?"*

LR-160　LR-60　VO-160　VO-60
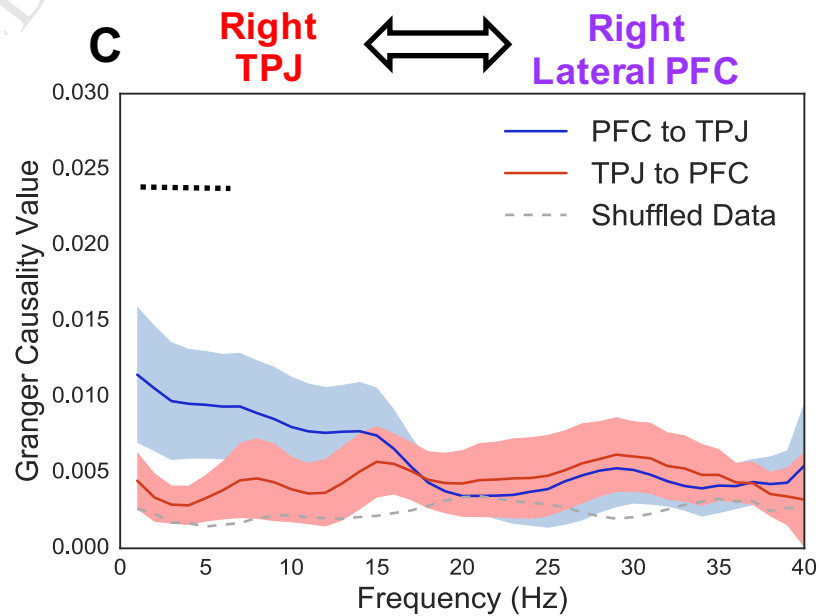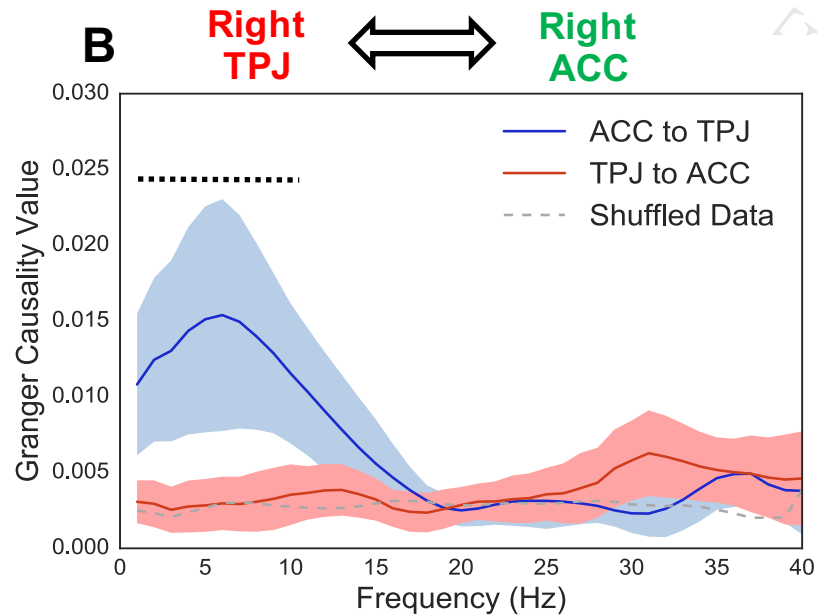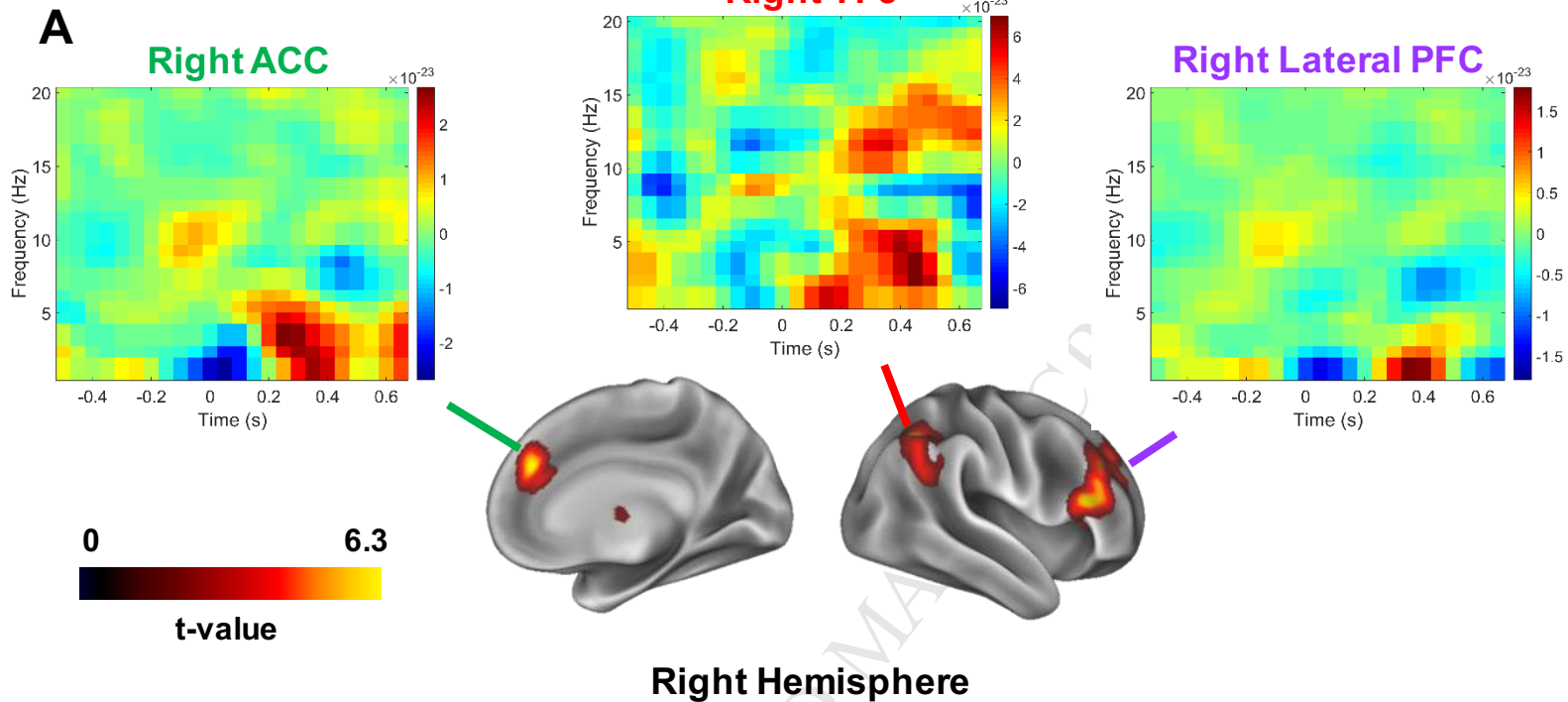
Left Hemisphere

Right Hemisphere

Intra-parietal Sulcus/ PPC

Supramarginal Gyrus/ SMC

Left Anterior Temporal Lobe (ATL)

Ventral Visual Stream

Left Posterior Cingulate Cortex/ SMA

Right Posterior Cingulate Cortex (PCC)

Medial PFC

Ventral Visual Stream / VOTC

-4.6   0   3.1

t-value

Executive Network:
Top-down Cognitive Control

| ACC | Lateral PFC |

Visual & Ventral Stream

rTPJ

| PCC |
| Medial PFC |
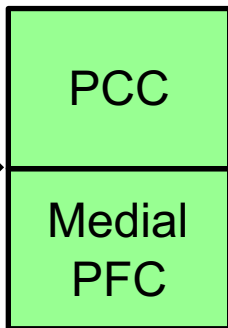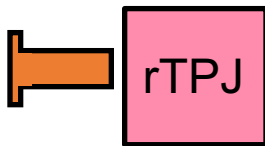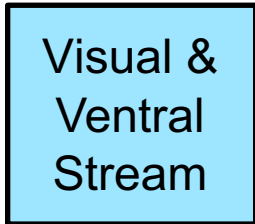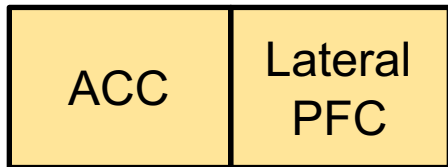
Theory of Mind Network:
Representations of Self vs. "Other"

| SMC | SMA | PPC |
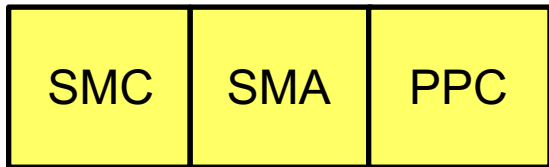
Motor/Body-Schema Network:
Embodied Transformation